Journal of Power Sources 197 (2012) 319–324

Contents lists available at SciVerse ScienceDirect

Journal of Power Sources

journal homepage: www.elsevier.com/locate/jpowsour

Polypyrrole/carbon nanotube nanocomposite enhanced the electrochemical capacitance of flexible graphene film for supercapacitors

Xiangjun Lu[a], Hui Dou[a,*], Changzhou Yuan[b], Sudong Yang[a], Liang Hao[a], Fang Zhang[a], Laifa Shen[a], Luojiang Zhang[a], Xiaogang Zhang[a,*]

[a] College of Material Science and Engineering, Nanjing University of Aeronautics and Astronautics, Nanjing 210016, PR China
[b] School of Materials Science and Engineering, Anhui University of Technology, Ma'anshan 243002, PR China

ARTICLE INFO

Article history:
Received 29 July 2011
Received in revised form 30 August 2011
Accepted 31 August 2011
Available online 6 September 2011

Keywords:
Graphene
Carbon nanotube
Polypyrrole
Supercapacitor
Flexible film

ABSTRACT

The flexible electrodes have important potential applications in energy storage of portable electronic devices for their powerful structural properties. In this work, unique flexible films with polypyrrole/carbon nanotube (PPy/CNT) composite homogeneously distributed between graphene (GN) sheets are successfully prepared by flow-assembly of the mixture dispersion of GN and PPy/CNT. In such layered structure, the coaxial PPy/CNT nanocables can not only enlarge the space between GN sheets but also provide pseudo-capacitance to enhance the total capacitance of electrodes. According to the galvanostatic charge/discharge analysis, the mass and volume specific capacitances of GN-PPy/CNT (52 wt% PPy/CNT) are 211 F g^{-1} and 122 F cm^{-3} at a current density of 0.2 A g^{-1}, higher than those of the GN film (73 F g^{-1} and 79 F cm^{-3}) and PPy/CNT (164 F g^{-1} and 67 F cm^{-3}). Significantly, the GN-PPy/CNT electrode shows excellent cycling stability (5% capacity loss after 5000 cycles) due to the flexible GN layer and the rigid CNT core synergistical releasing the intrinsic differential strain of PPy chains during long-term charge/discharge cycles.

1. Introduction

Recently, there has been great interest in flexible conversion/storage resources for applications in portable electronic devices, including high-performance sportswear, implantable medical devices, roll-up displays and active RFID tags/cards [1–5]. Nevertheless, the fabrication of flexible conversion/storage resources is limited to the lack of dependable materials, because important requirements for useful alternative materials in pliable electrodes include not only good mechanical flexibility and high conductivity but also excellent cycle capability. Since Geim and coworkers reported the fact that two-dimensional graphene (GN) is stable under ambient conditions [6], tremendous efforts have been devoted to explore the potential application of GN in energy storage [7–10]. Being an unrolled carbon nanotube (CNT), GN is regarded as one of the ideal candidates for flexible electrode materials due to its particularly structural, mechanical and electrical properties [11–13]. For instance, Kang et al. utilized GN film as a conducting agent and a current collector in fabrication of flexible lithium rechargeable battery [14]. However, owing to the face-to-face aggregation of GN sheets, directly assembling GN sheets into two-dimensional film is not appropriate for applying in supercapacitors that are an increasingly important class of electrochemical devices for storing and releasing energy reversibly and quickly [15–17].

As is well-known, the energy of the electrical double layer capacitors (EDLCs) only involves the electrostatic charge accumulation at the electrode/electrolyte interfaces, that is, the electrochemical capacitive performance of GN film strongly depends on the electrolyte-accessible surface area of GN sheets. One effective strategy to restrain the ordered stacking of GN sheets is using one-dimensional CNT as a nanospacer to form a three-dimensional hierarchical structure film, remarkably improving the utilization of GN [18–20]. Differ from EDLCs, pseudo-capacitors are related to the fast and reversible surface redox reactions for storing energy. Therefore, the combination of GN and pseudo-capacitive materials (such as transition metal oxides and conductive polymers) can provide the EDLCs at the electrode/electrolyte interfaces and the faradaic capacitors coming from the electroactive pseudo-capacitive species simultaneously. Films of GN/polyaniline (PANI) [21–25], GN/polypyrrole (PPy) [26,27] and GN/NiO [28] have been fabricated as active materials for supercapacitor electrodes by *in situ* chemical or electrochemical polymerization, in which GN acts as a substrate for depositing or immobilizing the pseudo-capacitive materials.

* Corresponding authors. Tel.: +86 025 52112918; fax: +86 025 52112626.
E-mail addresses: dh_msc@nuaa.edu.cn (H. Dou), azhangxg@nuaa.edu.cn (X. Zhang).

0378-7753/$ – see front matter © 2011 Elsevier B.V. All rights reserved.
doi:10.1016/j.jpowsour.2011.08.112

The capacity loss of the electrodes based on conducting polymers during the continuous charge/discharge processes is one of their most fatal shortages. Literature reviews of electrodes made from conducting polymers indicate that high stability should be obtained in principle [29–31]. Although the binary composites of conducting polymers with either flexible GN or rigid CNT have been demonstrated improvement in the electrochemical stability, there is no significant reinforcement among the previous reports for practical applications. For example, a capacity loss of 21% after 800 cycles for flexible GN/PANI electrode [22], a capacity loss of 11% after 1000 cycles for flexible CNT/PANI [32] and a capacity loss of 8% after 800 cycles for GN/PPy film [27] have been reported. To relieve the cycle degradation problem caused by volumetric change, recently, designing and developing hierarchically ternary composite materials composed of GN, CNT and conducting polymers have been explored [33,34]. The results show that the powdery ternary composites have excellent cycle stability due to the high mechanical properties of flexible GN and rigid CNT synergistical releasing intrinsic differential strain of polymer chains during doping/dedoping processes.

In the present study, a novel and facile strategy, for the first time, is proposed to prepare flexible GN-PPy/CNT ternary composite film with coaxial PPy/CNT nanocables uniformly sandwiched between the GN sheets through a flow-assembly method, in which the flexible GN layer and the rigid CNT core can improve the mechanical stability of PPy chains. New insights on the design of an ideal flexible electrode with high stability are provided.

2. Experimental

2.1. Chemicals and materials

Pyrrole (A.R., Shanghai Chemical Reagent Co. Ltd.) was purified through distillation under reduced pressure and stored refrigerated before use. The CNT was purchased from Nanotech Port Co. Ltd. (Shenzhen, China) and purified by refluxing the as-received CNT in nitric acid at 40 °C for 4 h. All other reagents used in our experiment were of analytical reagent grade and were used without further purification. Aqueous solutions were freshly prepared using high purity water (18 MΩ cm^{-1} resistance) from an Ampeon 1810-B system.

2.2. Preparation of water-dispersible PPy/CNT composite

A water-dispersible PPy/CNT composite was synthesized by *in situ* polymerization according to the literature [35]. 20 mg CNT and 0.2 g poly(sodium 4-styrenesulfonate) (PSS) were added to 100 mL water, followed by 2 h sonication to disperse CNT in solution. 0.1 g pyrrole was added and the mixture was stirred for 0.5 h. 0.34 g ammonium persulfate dissolved in 20 mL water was slowly added into the solution and polymerization was conducted at 0–5 °C with constant mechanical stirring for 4 h. The products were washed with water and ethanol by centrifuged, and dried at 50 °C for 24 h (the 24 wt% of CNT in PPy/CNT composite was evaluated by calculating the weight difference of CNT).

2.3. Preparation of GN-PPy/CNT and GN films

Graphite oxide (GO) was synthesized from natural graphite flakes by the modified Hummers method [36]. Aqueous GN dispersion was prepared by controlled chemical conversion of GO colloid developed by Li et al. [37]. The procedures are described briefly as follows. 30 mg GO was dispersed in 60 mL water by ultrasonic treatment for 1 h. Subsequently, 400 μL of ammonia solution (28 wt% in water) and 25 μL of hydrazine solution (85 wt% in water) were added into the GO dispersion. After being vigorously shaken for a few minutes, the mixture was stirred at 95 °C for 12 h. The resulting solution was dialyzed against ammonia solution (pH = 10) for 1 week. Finally, the black dispersion was then subjected to 10 min of centrifugation at 4000 rpm to remove aggregated GN sheets (presenting in a very small amount).

15 mg PPy/CNT dispersed in 10 mL ammonia solution (pH = 10) was added to the GN dispersion and then sonicated for 0.5 h. The resultant mixture dispersion of GN and PPy/CNT was filtered by a vacuum filter equipped with a 0.2-μm porous PTFE membrane to produce a GN-PPy/CNT film that was then dried under vacuum at room temperature for 24 h. The final mass of GN-PPy/CNT film was 28.8 mg (52 wt% of PPy/CNT) (named as GN-PPy/CNT52). GN film was fabricated by means of the same procedure described above. The average thicknesses of the GN and GN-PPy/CNT films were *ca.* 10.2 and 39.7 μm, respectively. Parallel experiments were carried out just by changing the amount of PPy/CNT in the starting mixture to obtain other GN-PPy/CNT composites with different mass ratio of PPy/CNT.

2.4. Material characterization

The morphology was characterized by scanning electron microscopy (SEM, LEO1530) and transmission electron microscopy (TEM, JEM-2100). X-ray diffraction (XRD) measurements were performed on a Bruker D8 advance-X diffractometer with Cu Kα radiation (λ = 1.5418 Å). Fourier transformation infrared (FTIR) spectra of the synthetic samples were recorded with a Model 360 Nicolet AVATAR. The specific surface area (SSA) was obtained by using a Micromeritics ASAP 2010 instrument. The samples were degassed for 4 h at 160 °C. The electrical conductivity was evaluated by a four-point probe meter.

2.5. Electrochemical measurement

Electrochemical performances were determined mainly by the cyclic voltammetry (CV) and galvanostatic charge/discharge (GCD) using a CHI 660 C electrochemical analyzer system in 1 M KCl aqueous solution, where the three electrode system was equipped with a platinum plate counter electrode and a saturated calomel electrode (SCE) reference electrode. The films (5 mg) connected by simple alligator clips were used as the working electrodes. The PPy/CNT working electrode for electrochemical measurement was fabricated by mixing PPy/CNT (5 mg) with polytetrafluoroethylene with the weight ratio of 9:1. A small amount of water was then added to the mixture and ground to form a homogeneous coating slurry that was smeared onto the graphite current collector (area: 1 cm × 1 cm) and dried at room temperature.

3. Results and discussion

3.1. Physicochemical characterization

As recently demonstrated in many literature results [18–23], the forming of hierarchically structured GN-based composite films is strongly dependent on the aqueous dispersibility of each component. It has been confirmed that the direct dispersion of hydrophobic GN sheets in water without the assistance of dispersing agents can be readily obtained by controlled chemical conversion of GO colloid [37]. On the other hand, PPy/CNT composite with well-dispersion in water also can be successfully synthesized by *in situ* chemical oxidation polymerization using PSS as a dispersing agent. The resulting mixture of well water-dispersible GN and PPy/CNT is convenient for the fabrication of a reasonably uniform film with ordered hierarchical structure under vacuum filtration. As shown in Fig. 1, the black GN-PPy/CNT52 film has good flexibility. The SEM of PPy/CNT is presented in Fig. 2, which

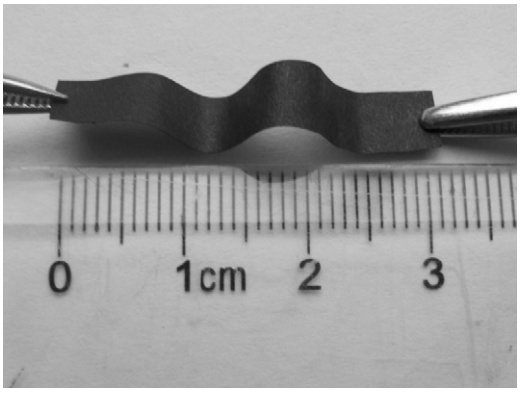

Fig. 1. Photograph of flexible GN-PPy/CNT film52.

shows that the CNT serves as template for the formation of one-dimensional PPy/CNT nanostructure. It is necessary to point out that the negatively charged PSS not only disperses the PPy/CNT composite in water but also favors the electrostatic attract to bind PPy chains onto CNT surface during the polymerization process [38]. As can be seen from the SEM images of cross-section in Fig. 3a and b, the GN-PPy/CNT52 film exhibits a layer-by-layer stacking structure and the coaxial PPy/CNT nanocables are sandwiched uniformly between the GN sheets. As shown in TEM image of GN-PPy/CNT52 in Fig. 3c, the PPy/CNT composite with one-dimensional core-shell structure distributes on the surface of GN sheet. For comparison, Fig. 3d and e shows the SEM images of cross-section of GN film. Obviously, tightly packed GN sheets are observed.

Fig. 4 shows the FTIR spectra of (a) GO, (b) GN, (c) PPy/CNT and (d) GN-PPy/CNT52. The main characteristic peaks of GO are assigned as follows: the peaks at 1057, 1224 and 3407 cm^{-1} are attributed to C–O–C, C–OH and O–H stretching vibrations, respectively. The peak at 1623 cm^{-1} is ascribed to aromatic C=C vibration

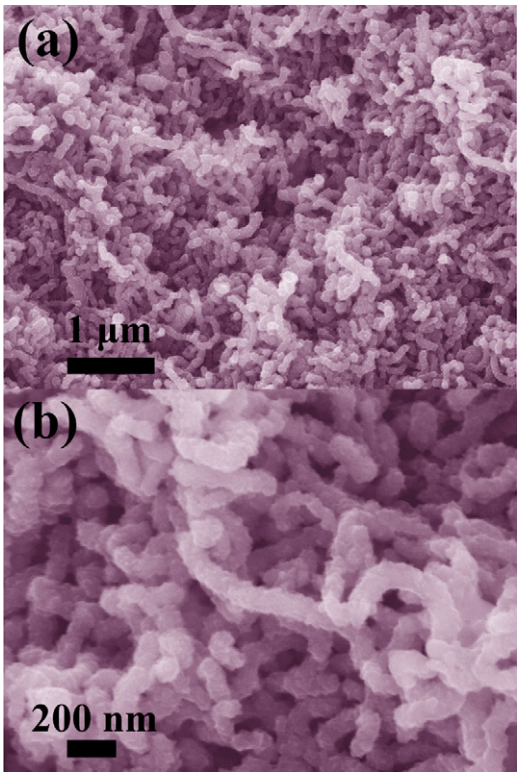

Fig. 2. SEM images of PPy/CNT.

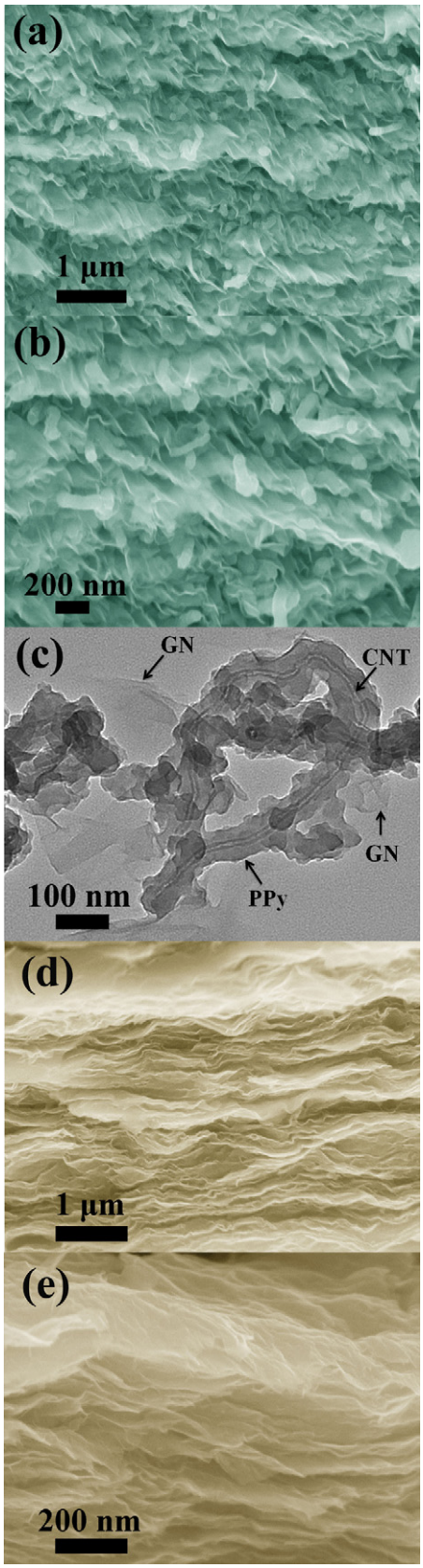

Fig. 3. SEM images of cross-section of (a and b) GN-PPy/CNT52 and (d and e) GN; (c) TEM image of GN-PPy/CNT52.

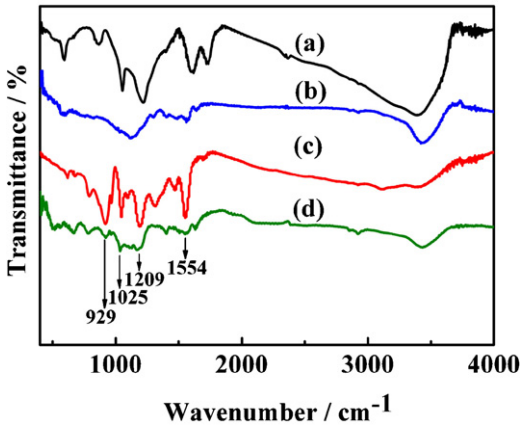

Fig. 4. FTIR spectra of (a) GO, (b) GN, (c) PPy/CNT and (d) GN-PPy/CNT52.

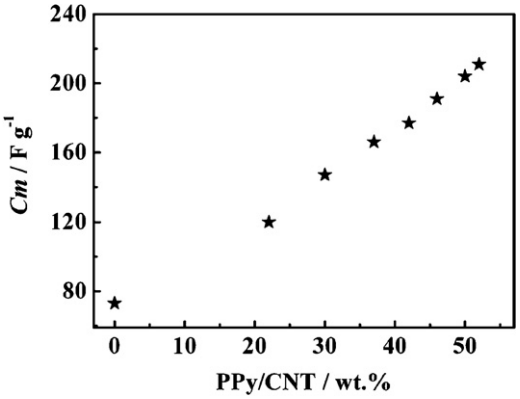

Fig. 6. The *C*m of GN-PPy/CNT composite film with different weight percent of PPy/CNT within the potential window −0.5 to 0.5 V at a current density of 0.2 A g^{-1} in 1 M KCl.

of unoxidized graphitic domains, while peak at 1728 cm^{-1} reflects C=O stretching motions of carboxylic acid and carbonyl moieties. The results are consistent with the literature values [39–41]. After reduction by hydrazine, the attenuating peaks at 1623 and 3407 cm^{-1} and the completely disappearing peaks at 1057, 1224 and 1728 cm^{-1} suggest that the most of functional groups have been removed. Compared with the corresponding characteristic peaks of GN, it can be seen that several new peaks attributed to PPy chains appear in the spectrum of GN-PPy/CNT52. The new peaks at 929, 1025, 1209 and 1554 cm^{-1} are attributed to C–H out-of-plane deformation vibration, C–H deformation and N–H stretching vibrations, C–N stretching vibration and antisymmetric ring-stretching vibration, respectively. Fig. 5 shows the XRD patterns of GO, GN, PPy/CNT and GN-PPy/CNT52. GO exhibits an intense and sharp peak centered at $2\theta = 11.5^\circ$, corresponding to the interplanar spacing of 0.78 nm of GO sheets. The as-filtrated GN film displays a broad XRD peak at around 25.6°, correlated to the layer-to-layer distance (*d*-spacing) of 0.35 nm of GN sheets. In the case of PPy/CNT, the peak at $2\theta = 26.2^\circ$ is ascribed to the (0 0 2) reflection of CNT. The XRD patterns of as-prepared GN-PPy/CNT52 are similar to those of GN due to the reflection overlapping of the GN and PPy/CNT.

3.2. Electrochemical characterization

The mass specific capacitance (C_m) can be calculated from the GCD curves based on the equations:

$$C_m = \frac{I \times \Delta t}{\Delta V}$$

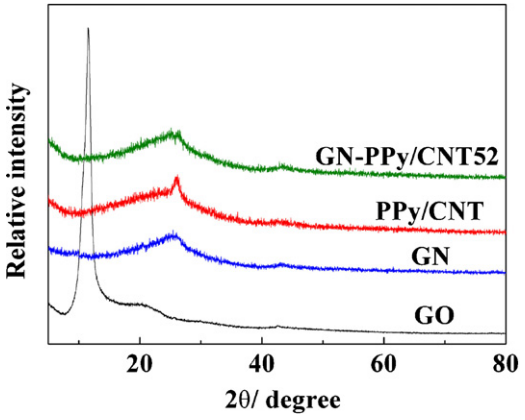

Fig. 5. XRD patterns of GO, GN, PPy/CNT and GN-PPy/CNT52.

where I (Ag^{-1}), Δt (s) and ΔV (V) represent the discharge current density, total discharge time and potential window during discharge, respectively. Fig. 6 shows the relationship between the C_m of GN-PPy/CNT composite and the weight percent of PPy/CNT. It is clear that the PPy/CNT nanocomposite could enhance the electrochemical capacitance of flexible GN film and there is an increase in the C_m of GN-PPy/CNT composite with increasing amount of PPy/CNT within the potential window −0.5 to 0.5 V at a current density of 0.2 A g^{-1}. The C_m of the composite can reach 211 F g^{-1} in the case of 52 wt% PPy/CNT (GN-PPy/CNT52). However, further increase on the weight percent of PPy/CNT results in the corresponding composite films fragile after drying. Therefore, the GN-PPy/CNT52 film and the contrast experiment of GN and PPy/CNT will be investigated in detail in the next section.

CV measurements were employed to investigate the electrochemical behaviors of GN, PPy/CNT and GN-PPy/CNT52. Fig. 7a shows the CV curves within potential range of −0.8 to 0.5 V in 1 M KCl electrolyte at a scan rate of 10 mV s^{-1}. For GN, the CV curve presents good mirror image and symmetric *I*–*E* response, which are typical of an ideal capacitive behavior. The CV curves of PPy/CNT and GN-PPy/CNT52 electrodes exhibit well-defined redox peaks that correspond to the doping and dedoping of electrolyte ions in the PPy chains during charge/discharge processes, suggesting that their capacitance characteristic is different from that of the EDLCs. From the CV curves, it can be observed that the GN-PPy/CNT52 has larger voltammetric current response compared with GN and PPy/CNT, revealing higher charge storage capability of GN-PPy/CNT52. For PPy/CNT and GN-PPy/CNT52, all the electrochemical oxidation and reduction response currents decrease towards the negative potential end due to the electroactive PPy gradually becoming inactive and resistive. However, compared with the PPy/CNT, the anodic and cathodic peak potentials of GN-PPy/CNT52 have about −0.2 V potential shift, indicating that the PPy in GN-PPy/CNT52 has good electroactive at low potential region. This can be attributed to the following reason. First, the presence of highly conjugated GN can increase the electron delocalization along the PPy chains to reduce its IR drop [42,43]. Second, the GN with negative charge [37] can function as the immobilized dopant anions to easier remove electrons and anions from the PPy chains during charge and discharge processes, respectively [44]. As the scan rate increases to 80 mV s^{-1} (Fig. 7b), the plot of PPy/CNT tends to present shuttle-shaped. The GN-PPy/CNT52 electrode exhibits significantly larger CV current than PPy/CNT and a pair of broad redox peaks at 0.24/−0.63 V (marked by arrows in Fig. 7b), indicating its good rate ability.

To further investigate the electrochemical characteristic of the resulting electrodes for supercapacitors, GCD measurements were

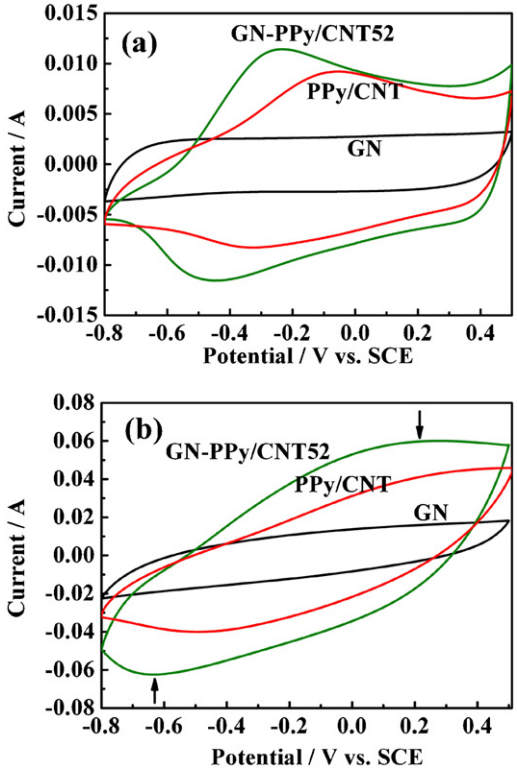

Fig. 7. CV curves of GN, PPy/CNT and GN-PPy/CNT52 within potential range of −0.8 to 0.5 V at scan rates of (a) 10 and (b) 80 mV s^{-1} in 1 M KCl.

performed at different current densities. Fig. 8 shows the GCD curves of GN, PPy/CNT and GN-PPy/CNT52 at a current density of 0.2 A g^{-1} with voltage between −0.5 and 0.5 V. Calculations based on the slopes of the discharge curve indicate that the GN-PANI/CNT52 film exhibits higher C_m (211 F g^{-1}) compared with that of GN film (73 F g^{-1}) and PPy/CNT (164 F g^{-1}). We noted that the C_m of powdery PPy/CNT composite in this work is smaller than that reported for PPy/CNT composites [45–47]. This is probably due to the existence of nonelectroactivity and insulating PSS in PPy/CNT composite. In addition, compared with the powdery GN/PANI/CNT ternary composites in the published literatures [33,34], the GN-PPy/CNT52 composite film shows a lower C_m, which can be attributed to relatively smaller theoretic capacitance of PPy (620 F g^{-1}) [29] than that of PANI (2000 F g^{-1}) [48]. The volumetric capacitance (C_v) also is an important parameter for supercapacitor electrodes, especially for flexible electrodes [22,24]. The density of GN-PPy/CNT52, GN and PPy/CNT is 0.58,

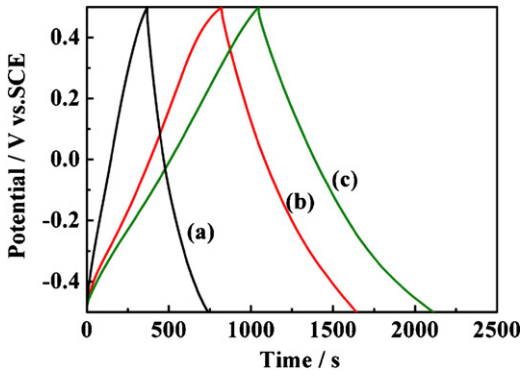

Fig. 8. GCD curves of (a) GN, (b) PPy/CNT and (c) GN-PPy/CNT52 with voltage between −0.5 and 0.5 V at a current density of 0.2 A g^{-1} in 1 M KCl.

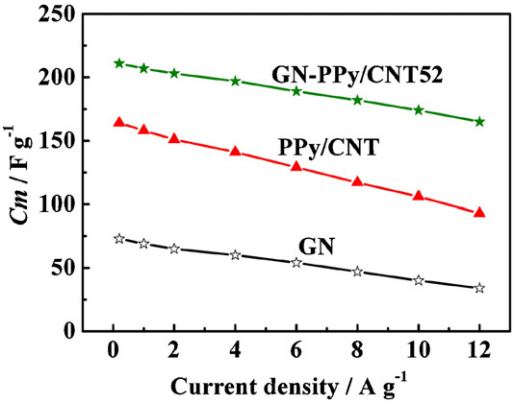

Fig. 9. C_m values of GN, PPy/CNT and GN-PPy/CNT52 at different current densities.

1.08 and 0.41 g cm^{-3}, respectively. The C_v value of GN-PPy/CNT52 electrode at 0.2 A g^{-1} is calculated to be 122 F cm^{-3}, much larger than that of GN (79 F cm^{-3}) and PPy/CNT (67 F cm^{-3}). To further understand the high rate capability of the sample electrodes, we plot the dependency of the calculated *C*m values of GN, PPy/CNT and GN-PPy/CNT52 on the current density. As shown in Fig. 9, although the capacitance of all electrodes decreases with growth of current density from 0.2 to 12 A g^{-1}, the capacitance retention rate of GN-PPy/CNT52 still reaches about 78%, higher than that of GN (47%) and PPy/CNT (57%), indicating that high capacitance of GN-PPy/CNT52 electrode can be maintained under high power operations.

The cycle ability of the electrodes in electrolyte is one of the important factors for their practical application. As shown in Fig. 10, the C_m of PPy/CNT decreases 45% (from 106 to 58 F g^{-1}) at a high current density of 10 A g^{-1} after 5000 charge/discharge cycles. The degradation in capacitance should mainly associate with the repetitive volumetric expansion/contraction of PPy chains during the continuous injection/rejection (charge/discharge) of electrolyte ions, deteriorating the charge distribution and conformation of π conjugated PPy chains [26]. However, the capacity loss of GN-PPy/CNT52 is only 5% after 5000 consecutive cycles, confirming the excellent cyclability of the GN-PPy/CNT electrode.

The energy storage characteristics of hierarchical GN-PPy/CNT52 ternary composite are schematically illustrated in Fig. 11. The novel structure has several advantages to exhibit outstanding performance for supercapacitor applications. Firstly, the functional material GN in the composite acts as not only active substrate for flexible electrode but also outer current collector. Therefore, for free-standing GN-PPy/CNT electrode, the insulating

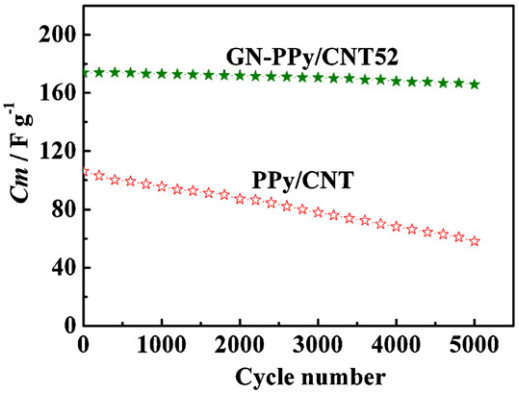

Fig. 10. Cycle life of PPy/CNT and GN-PPy/CNT52 at a current density of 10 A g^{-1}.

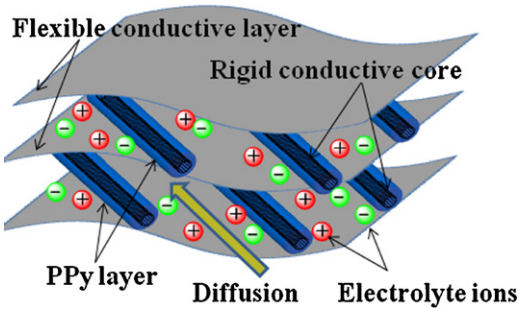

Fig. 11. Schematic representation of the microstructure and energy storage characteristics of the GN-PPy/CNT52 film.

binder that results in effective surface area loss and adds extra contact resistance, is not necessary. Secondly, the PPy layer depositing on the surface of CNT provides pseudo-capacitance to increase the total capacitance of the electrode. Thirdly, the PPy/CNT nanocables function as spacers to restrain the closely restacking of GN sheets, enhancing the EDLCs of the GN sheets. This can be verified by the SSA of 98 $m^2\,g^{-1}$ for the GN-PPy/CNT52 composite, as compared with that of the GN film (37 $m^2\,g^{-1}$). After deducting the SSA of PPy/CNT (41 $m^2\,g^{-1}$), the SSA of GN sheets in GN-PPy/CNT52 film is 160 $m^2\,g^{-1}$. Fourthly, the pseudo-active PPy layer is contacted directly with the outer current collector of GN and inner conductible core of CNT, thus this conducting three-dimensional nano-network enables fast charge and ion transportation, especially at high current densities (the electrical conductivity of GN, GN-PPy/CNT52 and PPy/CNT is 24.4, 15.3 and 6.1 $S\,cm^{-1}$ at room temperature, respectively). In addition, the flexible GN can act as strain buffer for volume swelling/shrinkage of the PPy chains during the electrochemical reaction, and the rigid CNT core can transfer the strain associated with the volume change due to the π-π interaction between CNT and heterocyclic PPy [49].

4. Conclusions

To recapitulate, we propose for the first time a facile strategy for generating flexible GN-PPy/CNT ternary composite film. Working as supercapacitors, the flexible conducting GN layer and the rigid conducting CNT core allow for efficient charge and ion transport, improve the electronic conductivity of the composite significantly and synergistically release the intrinsic differential strain of PPy chains during charge/discharge processes. The *C*m and *C*v of the GN-PPy/CNT52 composite (211 $F\,g^{-1}$ and 122 $F\,cm^{-3}$) is higher than those of the GN (73 $F\,g^{-1}$ and 79 $F\,cm^{-3}$) and PPy/CNT (164 $F\,g^{-1}$ and 67 $F\,cm^{-3}$) at a discharge current of 0.2 $A\,g^{-1}$. In addition, the free-standing GN-PPy/CNT52 film has good charge/discharge rate (78% capacity retention at 12 $A\,g^{-1}$) and excellent cycling stability (5% capacity loss after 5000 cycles). Based on the above results, such GN-PPy/CNT52 film is very promising for flexible energy storage devices.

Acknowledgements

This work was supported by National Basic Research Program of China (973 Program) (No. 2007CB209703) and National Natural Science Foundation of China (No. 20873064).

References

[1] M. Kaltenbrunner, G. Kettlgruber, C. Siket, R. Schwödiauer, S. Bauer, Adv. Mater. 22 (2010) 2065–2067.
[2] P. Hiralal, S. Imaizumi, H.E. Unalan, H. Matsumoto, M. Minagawa, M. Rouvala, A. Tanioka, G.A.J. Amaratunga, ACS Nano 4 (2010) 2730–2734.
[3] L.B. Hu, M. Pasta, F. La-Mantia, L.F. Cui, S. Jeong, H.D. Deshazer, J.W. Choi, S.M. Han, Y. Cui, Nano Lett. 10 (2010) 708–714.
[4] K.T. Nam, D.W. Kim, P.J. Yoo, C.Y. Chiang, N. Meethong, P.T. Hammond, Y.M. Chiang, A.M. Belcher, Science 312 (2006) 885–888.
[5] M. Rasouli, L.S.J. Phee, Expert Rev. Med. Devices 7 (2010) 693–709.
[6] K.S. Novoselov, A.K. Geim, S.V. Morozov, D. Jiang, Y. Zhang, S.V. Dubonos, I.V. Grigorieva, A.A. Firsov, Science 306 (2004) 666–669.
[7] M.D. Stoller, S.J. Park, Y.W. Zhu, J.H. An, R.S. Ruoff, Nano Lett. 8 (2008) 3498–3502.
[8] Y. Wang, Z.Q. Shi, Y. Huang, Y.F. Ma, C.Y. Wang, M.M. Chen, Y.S. Chen, J. Phys. Chem. C 113 (2009) 13103–13107.
[9] W. Lv, D.M. Tang, Y.B. He, C.H. You, Z.Q. Shi, X.C. Chen, C.M. Chen, P.X. Hou, C. Liu, Q.H. Yang, ACS Nano 3 (2009) 3730–3736.
[10] Y.W. Zhu, S. Murali, M.D. Stoller, A. Velamakanni, R.D. Piner, R.S. Ruoff, Carbon 48 (2010) 2118–2122.
[11] H.K. Chae, D.Y. Siberio-Perez, J. Kim, Y. Go, M. Eddaoudi, A.J. Matzger, M. O'Keeffe, O.M. Yaghi, Nature 427 (2004) 523–527.
[12] C.G. Lee, X.D. Wei, J.W. Kysar, J. Hone, Science 321 (2008) 385–388.
[13] C.N.R. Rao, A.K. Sood, K.S. Subrahmanyam, A. Govindaraj, Angew. Chem. Int. Ed. 48 (2009) 7752–7778.
[14] H. Gwon, H.S. Kim, K.U. Lee, D.H. Seo, Y.C. Park, Y.S. Lee, B.T. Ahn, K. Kang, Energy Environ. Sci. 4 (2011) 1277–1283.
[15] Y.Q. Sun, Q. Wu, G.Q. Shi, Energy Environ. Sci. 4 (2011) 1113–1132.
[16] S. Biswas, L.T. Drzal, ACS Appl. Mater. Interface 2 (2010) 2293–2300.
[17] Y.X. Xu, G.Q. Shi, J. Mater. Chem. 21 (2011) 3311–3323.
[18] D.S. Yu, L.M. Dai, J. Phys. Chem. Lett. 1 (2010) 467–470.
[19] L. Qiu, X.W. Yang, X.L. Gou, W.R. Yang, Z.F. Ma, G.G. Wallace, D. Li, Chem. Eur. J. 16 (2010) 10653–10658.
[20] X.J. Lu, H. Dou, B. Gao, C.Z. Yuan, S.D. Yang, L. Hao, L.F. Shen, X.G. Zhang, Electrochim. Acta 56 (2011) 5115–5121.
[21] X.B. Yan, J.T. Chen, J. Yang, Q.J. Xue, P. Miele, ACS Appl. Mater. Interface 2 (2010) 2521–2529.
[22] Q. Wu, Y.X. Xu, Z.Y. Yao, A.R. Liu, G.Q. Shi, ACS Nano 4 (2010) 1963–1970.
[23] S. Liu, X.H. Liu, Z.P. Li, S.R. Yang, J.Q. Wang, New J. Chem. 35 (2011) 369–374.
[24] D.W. Wang, F. Li, J.P. Zhao, W.C. Ren, Z.G. Chen, J. Tan, Z.S. Wu, I. Gentle, G.Q. Lu, H.M. Cheng, ACS Nano 3 (2009) 1745–1752.
[25] X.M. Feng, R.M. Li, Y.W. Ma, R.F. Chen, N.E. Shi, Q.L. Fan, W. Huang, Adv. Funct. Mater. 21 (2011) 2989–2996.
[26] S. Biswas, L.T. Drzal, Chem. Mater. 22 (2010) 5667–5671.
[27] A.R. Liu, C. Li, H. Bai, G.Q. Shi, J. Phys. Chem. C 114 (2010) 22783–22789.
[28] W. Lv, F. Sun, D.M. Tang, H.T. Fang, C. Liu, Q.H. Yang, H.M. Cheng, J. Mater. Chem. 21 (2011) 9014–9019.
[29] G.A. Snook, P. Kao, A.S. Best, J. Power Sources 196 (2011) 1–12.
[30] H. Zhang, G.P. Cao, Y.S. Yang, Energy Environ. Sci. 2 (2009) 932–943.
[31] C. Peng, S.W. Zhang, D. Jewell, G.Z. Chen, Prog. Nat. Sci. 18 (2008) 777–788.
[32] C.Z. Meng, C.H. Liu, S.S. Fan, Electrochem. Commun. 11 (2009) 186–189.
[33] J. Yan, T. Wei, Z.J. Fan, W.Z. Qian, M.L. Zhang, X.D. Shen, F. Wei, J. Power Sources 195 (2010) 3041–3045.
[34] K.S. Kim, S.J. Park, Electrochim. Acta 56 (2011) 1629–1635.
[35] T.M. Wu, H.L. Chang, Y.W. Lin, Compos. Sci. Technol. 69 (2009) 639–644.
[36] W.S. Hummers, R.E. Offeman, J. Am. Chem. Soc. 80 (1958) 1339.
[37] D. Li, M.B. Muller, S. Gilje, R.B. Kaner, G.G. Wallace, Nat. Nanotechnol. 3 (2008) 101–105.
[38] R.K. Sharma, A. Karakoti, S. Seala, L. Zhai, J. Power Sources 195 (2010) 1256–1262.
[39] H.L. Wang, Q.L. Hao, X.J. Yang, L.D. Lu, X. Wang, Electrochem. Commun. 11 (2009) 1158–1161.
[40] C.P. Tien, H.S. Teng, J. Power Sources 195 (2010) 2414–2418.
[41] J.J. Xu, K. Wang, S.Z. Zu, B.H. Han, Z.X. Wei, ACS Nano 4 (2010) 5019–5026.
[42] B. Gao, C.Z. Yuan, L.H. Su, S.Y. Chen, X.G. Zhang, Electrochim. Acta 54 (2009) 3561–3567.
[43] Y.G. Wang, L. Yu, Y.Y. Xia, J. Electrochem. Soc. 153 (2006) A743–A748.
[44] C. Peng, J. Jin, G.Z. Chen, Electrochim. Acta 53 (2007) 525–537.
[45] J.Y. Kim, K.H. Kim, K.B. Kim, J. Power Sources 176 (2008) 396–402.
[46] Y.P. Fang, J.W. Liu, D.J. Yu, J.P. Wicksted, K. Kalkan, C.O. Topal, B.N. Flanders, J. Wu, J. Li, J. Power Sources 195 (2010) 674–679.
[47] J. Wang, Y.L. Xu, X. Chen, X.F. Sun, Compos. Sci. Technol. 67 (2007) 2981–2985.
[48] H.L. Li, J.X. Wang, Q.X. Chu, Z. Wang, F.B. Zhang, S.C. Wang, J. Power Sources 190 (2009) 578–586.
[49] M. Foroutan, A.T. Nasrabadi, J. Phys. Chem. B 114 (2010) 5320–5326.